Journal of Information Processing Vol. 16 190–200 (Dec. 2008)

Regular Paper

A New 3D Shape Retrieval Method Using Spherical Healpix

Zhenbao Liu,[†1] Jun Mitani,[†1] Yukio Fukui[†1] and Seiichi Nishihara[†1]

Rapidly spreading 3D shape applications have led to the development of content-based 3D shape retrieval research. In this paper, we propose a new retrieval method using Spherical Healpix. Spherical Healpix is a new framework for efficient discretization and fast analysis or synthesis of functions defined on the sphere. We analyzed the construction process of this structure and defined a new Spherical Healpix Extent Function. We then analyzed this Spherical Healpix Extent Function using an inverse-construction process from the sphere to the Euclidean plane. We transformed the result of inverse-construction to the frequency domain using a 2D Fourier transform, instead of spherical harmonics, a well-known tool in spherical analysis. We obtained the low-frequency component in the frequency domain by using a Butterworth low-pass filter. The power spectrum of the low frequency component can be used as the feature vector to describe a 3D shape. This descriptor is extracted in the canonical coordinate frame; that is, each 3D-model is first normalized. We have examined this method on the Konstanz Shape Benchmark and SHREC data set, and confirmed its efficiency. We also compared this method with other methods on the same Konstanz Shape Benchmark and SHREC data set and evaluated the shape retrieval performance.

1. Introduction

Over the past years, researchers have made considerable efforts to make computers learn to understand, index, and retrieve texts and images representing a wide range of concepts. With the rapidly increasing use of 3D data, a relatively new data form, in many applications such as computer games, computer aided design, virtual reality environments, biology, e-business, etc., 3D shape data have a higher dimension and represent more complex human intelligence. Consequently, it is becoming challenging to describe and match these data. It is difficult for computers to finish these tasks although any human could recognize and distinguish them easily; accordingly, there is an increasing need to develop computer algorithms that enable people to find their interesting 3D shape data and discover relationships between them. Recently, much effort has been focused on developing techniques for efficient content-based retrieval of 3D objects [1),2)]. The key to content-based 3D shape matching and retrieval is to develop or find a simple mathematical descriptor capturing and extracting the main feature of 3D object, since 3D shapes can be discriminated by measuring and comparing these feature descriptors. In fact, feature extraction is a process that involves reducing the dimensions of the data from high-dimensional 3D data to low dimensional feature data. Moreover, the low dimensional feature can be used instead without any loss. The feature descriptors should have a high ability to distinguish and should be easily comparable, for example, it could match two shapes only to subtract two descriptors. If this could be done, the matching and retrieval algorithm could be realized in the computer.

We present a 3D shape retrieval method based on Spherical Healpix (**H**ierarchical **E**qual **A**rea iso-**L**atitude **Pix**elization) [4)]. We utilized the internal mechanism of Spherical Healpix in our method. We developed a new Spherical Healpix Extent Function, projected it by inverse-construction of Spherical Healpix, and analyzed it in the frequency domain by taking two dimensional Fourier transform and using a Butterworth low pass filter. The low frequency part is extracted for matching. We tested this method on a recently developed benchmark database, Konstanz Shape Benchmark [2),3)] and SHREC data set [24)], and evaluated the efficiency. We also compared our method with four other methods and evaluated the present method.

The outline of the remainder of the paper is as follows: in the next section we briefly review the previous studies on 3D model retrieval and relevant methods. In Section 3 we describe the method that we developed for feature computation. We will put emphasis on internal mechanism analysis of Spherical Healpix and how to apply Spherical Healpix to our feature computation. Section 4 describes the feature vector and similarity metric computations employed for feature matching. Section 5 gives the experimental results and Section 6 presents the conclusions of the study.

†1 Department of Computer Science, University of Tsukuba

2. Previous Work

In this section, we discuss recent 3D retrieval methods and classify them into two broad categories for shape matching, namely, feature distribution and shape descriptors. In the end, we also introduce the other relevant developments.

2.1 Feature Distribution

It is fast and easy to compare the feature distributions of models, since it makes some data statistics on elements of shape. Osada, et al. [5] match 3D models with histograms of Euclidean distances between two random points on the shape surface and use these to measure the global geometric properties of the object. They called the global geometric property D2 shape function. Another method developed by Ohbuchi, et al. [6] extends the D2 shape function by considering the inner product of the normals of sampled point pairs. Ankerst, et al. [7] used shape histograms decomposing shells and sectors around a model's centroid. Liu, et al. [8] utilize the directional histogram model to characterize 3D shapes. The shape can be described by the thickness distribution in the directions per latitude and longitude. Ohbuchi, et al. [9] perform the shape analysis by using the moments of inertia about the principal axes of the model. Liu, et al. [10] present a novel 3D shape descriptor for effective shape matching and analysis that utilizes both local and global shape signatures. They termed this descriptor "generalized shape distributions" since it is an extension of shape distributions [5]. All the feature distribution methods have a common limitation that they are capable of only capturing similar gross shape properties, and are powerless to capture the detailed shape properties.

2.2 Shape Descriptors

As a representative example, spherical harmonics [11] is applied in a wide variety of fields including earth physics, image analysis, and biology. It was first introduced in the 3D model retrieval by Vranic in Ref. 12). Funkhouser, et al. [13] presented a rotational invariant descriptor based on spherical harmonics. Vranic [14] improved this method [13] by combining it with Ref. 12). Saupe [15] constructed a moment-based descriptor by representing a spherical function using spherical harmonics. Feature extraction is performed using a rendered perspective projection of the object on an enclosing sphere [16]. It is considered as a shading-based shape descriptor. Novotni and Klein [17] present a 3D Zernike descriptor by computing 3D Zernike descriptors from voxelized models as natural extensions of spherical harmonics based descriptors. Liu, et al. [25] applied the multiresolution wavelet analysis on shape orientation for 3D shape retrieval.

2.3 Other Related Developments

Podolak, et al. [18] describe a planar reflective symmetry transform that captures a continuous measure of the reflectional symmetry of a shape with respect to all possible planes. The symmetry transform is useful for shape matching. Bespalov, et al. [19] presented several distinctive benchmark datasets for evaluating techniques for automated classification and retrieval of CAD objects.

In this present paper, we compare our method with four typical methods, shape distributions [5] and shape histograms on shells and sectors [7] — the two methods in feature distribution, rotational invariant spherical harmonics [13] and rays with spherical harmonics [12),14] — the other two methods about shape descriptors.

3. Feature Computation

In this section, we will focus on analyzing the internal mechanism of Spherical Healpix, and combining it with our new proposal to compute the feature of 3D shape.

3.1 Pose Estimation

As the first step, we use Principle Component Analysis (PCA) [20)–22)] to determine the invariant measure with respect to translation, rotation, reflection and scaling of the original shape. In the PCA method, we should point out that the covariance matrix is approximated as follows

$$C_I = \frac{1}{n}\sum_{i=1}^{n} S_i(g_i - m_I)(g_i - m_I)^T \quad (1)$$

Where S_i and g_i is the area of a triangle of a shape, and the center of gravity respectively, and m_I is the center of gravity of a shape, and n is the number of triangles of the shape.

3.2 Spherical Healpix

Healpix, **H**ierarchical **E**qual **A**rea iso-**L**atitude **Pix**elization, is a genuinely curvilinear partition of the sphere into exactly equal area quadrilaterals of varying

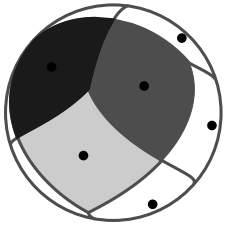

Fig. 1 Spherical Healpix [4].

shape. The base-resolution consists of twelve base pixels (see **Fig. 1**).

The resolution is expressed by the parameter N_s that defines the number of divisions along the side of a base-resolution pixel that is required to reach a desired high-resolution partition. According to N_s resolution, the spherical grid can produce N_p sampling points.

$$N_p = 12N_s^2 \tag{2}$$

Every point belongs to a partition, which has an area S_p that is equal to that of all the other partitions.

$$S_p = \frac{\pi}{3N_s^2} \tag{3}$$

3.3 The Construction Process

We analyze the construction process in which one projection scheme exists from Euclidean plane coordinate $(x,\ y)$ to spherical coordinate (θ, ϕ).

Given a grid resolution parameter N_s, for each base resolution pixel (face), use $(x,\ y)$ coordinates (index) in the Euclidean Plane to construct a square (where $x \in [0, N_s - 1]$, and $y \in [0, N_s - 1]$). The black points on the left plane in **Fig. 2** are $(x,\ y)$ coordinates, actually indices. Map the square to a sphere by using the following equations.

$$\begin{cases} i = F_1(f)N_s - (x+y) - 1 \\ j = \dfrac{F_2(f)N_s + (x-y) + s}{2} \end{cases} \tag{4}$$

Here $i \in [1, 4N_s - 1]$ is the index of iso-latitude ring of the sphere and j is the index of pixel in this ring. And f is the base-resolution pixel (face) index number

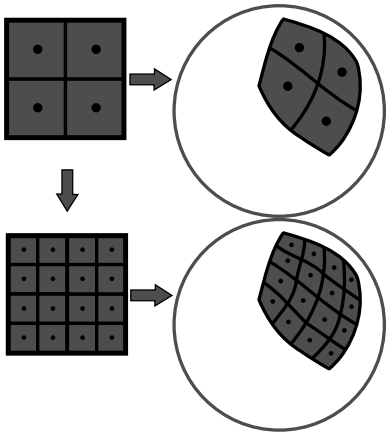

Fig. 2 Construction of Spherical Healpix.

running in $[0, 11]$. The two functions $F_1(f)$ and $F_2(f)$ index the location of the southernmost vertex of each base resolution pixel (face), and $s \in \{0, 1\}$ is an auxiliary index, describing phase shifts of the index j along iso-latitude rings. From two indices i and j, compute the corresponding spherical angular $(\theta_i,\ \phi_j)$ using the two following equations. This spherical angular $(\theta_i,\ \phi_j)$ could fix the black points on the right sphere in Fig. 2.

When $i \in \{[1, N_s - 1] \cup [3N_s + 1, 4N_s - 1]\}$,

$$\begin{cases} i' = i,\ i \in [1, N_s - 1] \\ i' = 4N_s - i,\ i \in [3N_s + 1, 4N_s - 1] \end{cases}$$

$$\begin{cases} \theta_i = \cos^{-1}\left(1 - \dfrac{i'^2}{3N_s^2}\right) \\ \phi_j = \dfrac{\pi}{2i'}\left(j - \dfrac{s}{2}\right) \end{cases} \tag{5}$$

When $i \in [N_s, 3N_s]$,

$$\begin{cases} i' = i,\ i \in [N_s, 2N_s] \\ i' = 4N_s - i,\ i \in [2N_s + 1, 3N_s] \end{cases}$$

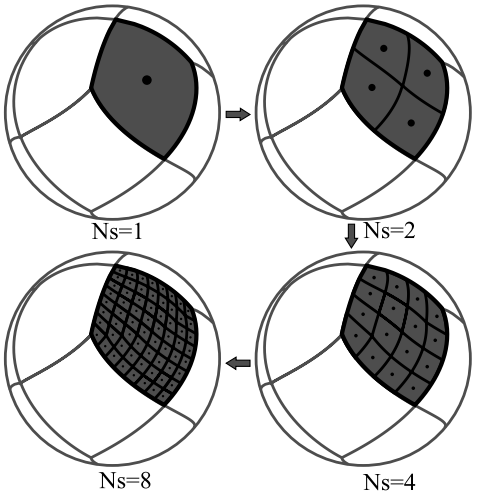

Fig. 3 Grid resolution of one face in Spherical Healpix [4].

$$\begin{cases} \theta_i = \cos^{-1}\left(\dfrac{4}{3} - \dfrac{2i'}{3N_s}\right) \\ \phi_j = \dfrac{\pi}{2N_s}\left(j - \dfrac{s}{2}\right) \end{cases} \tag{6}$$

Figure 2 depicts the constructing process of one face (In total 12 faces) from Euclidean plane to the light-gray region on the sphere. A higher resolution can be achieved by increasing N_s in the Euclidean plane and then projecting onto the sphere to form a finer Spherical Healpix structure.

In **Fig. 3**, the grid is hierarchically subdivided (clockwise from the upper-left panel) with a grid-resolution parameter $N_s = 1$, 2, 4, 8 and the total number of sampling $N_p = 12$, 48, 192, 768. The black points represent the sampling results.

3.4 The Problem with Conventional Spherical Extent Function

In the analysis of a discretized function on a sphere (e.g., spherical harmonics, spherical convolutions, spherical wavelet decomposition, and spherical topology), the spherical sampling exerts a strong influence.

In the common sampling stage, the spherical function is sampled using an $n \times n$ spherical grid defined in terms of the latitudinal and longitudinal angles (θ, ϕ). The sampling intervals on latitudinal and longitudinal angles are $\Delta\theta$ and $\Delta\phi$. This uniform sampling scheme has one major problem that the number of sampling points near the south and north poles is larger than that near the equator. As a result, some areas are over-sampled and other areas are under-sampled. This problem shows that the sampling is regular in spherical coordinate, but not in the Euclidean coordinate.

The Spherical Healpix projection is a good solution to this problem.

Table 1 Parameters of two extent functions.

N_s	S	B	$2B \times 2B$
8	768	32	4096
16	3072	64	16384
32	12288	128	65536

3.5 Spherical Healpix Extent Function

We defined a new spherical extent function based on Spherical Healpix.

Firstly, we divided the sphere into 12 faces according to the Healpix base solution pixels.

$$f_0, f_1, \ldots, f_k, \ldots f_{11}, \quad k \in [0, 11] \tag{7}$$

At a resolution level N_s, each face contains $N_s \times N_s$ sampling points. Rays extend along the directions (θ_i, ϕ_j) (Eqs. (5) and (6)) of the sampling points from the center of gravity of one 3D shape and intersect with the shape's surface. The farthest distance $d_{k,i,j}$ represents the spherical extent of the 3D shape.

The new spherical extent function can be defined as:

$$f_k(\theta_i, \phi_j) = d_{k,i,j}, \quad i, j \in [0, N_s - 1] \tag{8}$$

In our method, we employed three different resolutions of Spherical Healpix; the corresponding total sampling points S of Spherical Healpix extent function, and sampling rate of the conventional spherical extent function are given in **Table 1**. The sampling rate of the conventional spherical extent function is $2B \times 2B$ as follows, and B should be large enough ($B \geq 32$) to ensure that sufficient information about one object can be captured.

$$\theta_i = (2i + 1)\pi/2B, \quad \phi_j = j\pi/B, \quad i, j \in [0, 2B - 1].$$

3.6 Analysis of Spherical Healpix Extent Function

In our 3D shape retrieval method, we propose a new analysis method for the Spherical Healpix extent function.

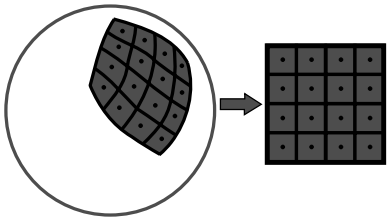

Fig. 4 Inverse-construction of Spherical Healpix.

Spherical harmonics cannot be directly used to analyze the Spherical Healpix extent function since the sampling of Spherical Healpix is irregular in the spherical coordinates.

We devised a new scheme that uses the inverse-construction of Spherical Healpix to analyze Spherical Healpix extent function.

For the extent function $f_k(\theta_i, \phi_j) = d_{k,i,j}$, i, $j \in [0, N_s - 1]$, we projected each face (e.g., one light-gray face in **Fig. 4**) to the Euclidean plane, and were able to construct a (x, y) plane function without information loss by exploiting the property of Spherical Healpix. The mapping relation is as follows.

$$\begin{cases} (\theta_i, \phi_j) \to (x, y) \\ f_k(\theta_i, \phi_j) \to f_k(x, y) \end{cases} \tag{9}$$

The correspondence relation is the same as that for the construction process. Here, x, $y \in [0, N_s - 1]$, and $k \in [0, 11]$.

The function is defined as follows.

$$f_k(x, y) = d_{k,x,y} \tag{10}$$

Since the new mapping function $f_k(x, y)$ is regularly distributed in the Euclidean plane, we will analyze it by firstly transforming the data into the frequency domain using the conventional method, namely, by taking 2D Fourier transform.

The 2D Fourier Transform is defined as

$$F_k(u, v) = \iint f_k(x, y) \exp(-j2\pi(ux + vy))dxdy \tag{11}$$

And its discrete form is given by

Table 2 Filter parameters.

n	8	16	32		
D_0	$n/2$	$n/4$	$n/6$	$n/8$	
σ	1	2	3	4	5

$$F_k(u, v) = \frac{1}{N_s^2} \sum_{x=0}^{N_s-1} \sum_{y=0}^{N_s-1} f_k(x, y) \exp\left(-j2\pi \frac{(ux + vy)}{N_s}\right),$$
$$u, v \in [0, n - 1]. \tag{12}$$

Here $F_k(u, v)$ represents the function in the frequency domain, and its center of frequency is $(u, v) = (n/2, n/2)$. We choose $n = N_s$, and adopt the 2D Fast Fourier Transform algorithm for reducing the computation time.

$|F(u, v)|$ is denoted as the power spectrum of $f(x, y)$.

3.7 Frequency Domain Analysis

To obtain low frequency components and filter high frequency components, we apply a filter to the frequency domain function.

$$G(u, v) = H(u, v)F(u, v) \tag{13}$$

Where $H(u, v)$ is a filter function. We chose Butterworth low pass filter [23] as the filter, it is described by

$$H(u, v) = \frac{1}{1 + [D(u, v)/D_0]^{2\sigma}} \tag{14}$$

Where D_0 is the cut-off frequency, and σ is the order.

$$D(u, v) = [(u - n/2)^2 + (v - n/2)^2]^{1/2} \tag{15}$$

In experiments, we adopt the parameter values given in **Table 2** and test these parameters for finding the best result.

4. Feature Vector and Similarity Metric

Finally, the power spectrum $|G(u, v)|$ is computed for the feature vector of the 3D shape.The degree of dissimilarity between two 3D shapes can be measured using the deviation between two corresponding feature vectors V_1 and V_2. We applied the following three metrics.

(1) L_1 Distance Metric

$$D = \|V_1 - V_2\| = \sum_{k=0}^{11}\sum_{i=0}^{n-1}\sum_{j=0}^{n-1}|v_{1,k,i,j} - v_{2,k,i,j}| \quad (16)$$

(2) L_2 Distance Metric

$$D = \|V_1 - V_2\|_2 = \left(\sum_{k=0}^{11}\sum_{i=0}^{n-1}\sum_{j=0}^{n-1}(v_{1,k,i,j} - v_{2,k,i,j})^2\right)^{\frac{1}{2}} \quad (17)$$

(3) Similarity Relation Metric

$$D = 1 - (V_1 \cdot V_2)/\left(\|V_1\|\ \|V_2\|\right) \quad (18)$$

After testing, we found that the L_1 Distance Metric gave the best retrieval results and it could be fit for comparison in the frequency domain.

5. Experiment Results

5.1 Retrieval Results

We show some examples of our retrieval results on the Konstanz Shape Benchmark. Firstly, we chose several sets of 3D shapes randomly including bottles, dogs, chairs, helicopters, humans and plants. From any set, given one shape as a query, **Table 3** represents the five most similar objects with the query orderly.

5.2 Experiment Means

We firstly chose the Konstanz Shape Benchmark for this experiment because this benchmark contains a considerable number of 3D shapes, in total 1,838 3D objects. From this set of 3D shapes, 472 objects were classified into 55 different model classes including animals, transportation tools, furniture, humans, plants, etc., and the remainder of the objects were left as unclassified. The unclassified objects can impact the evaluation result as a strong noise.

We chose two parameters to evaluate the performance, the Recall-Precision (R-P) Curves and the Average Recall-Precision (R-P).

Recall-Precision Curves (R-P Curves) have been used extensively in 3D retrieval methods. The precision is defined as the fraction of the objects relevant to the input query, and the recall is given by the fraction of retrieved objects from the test database.

Table 3 Retrieval examples using our method for the Konstanz Shape Benchmark.

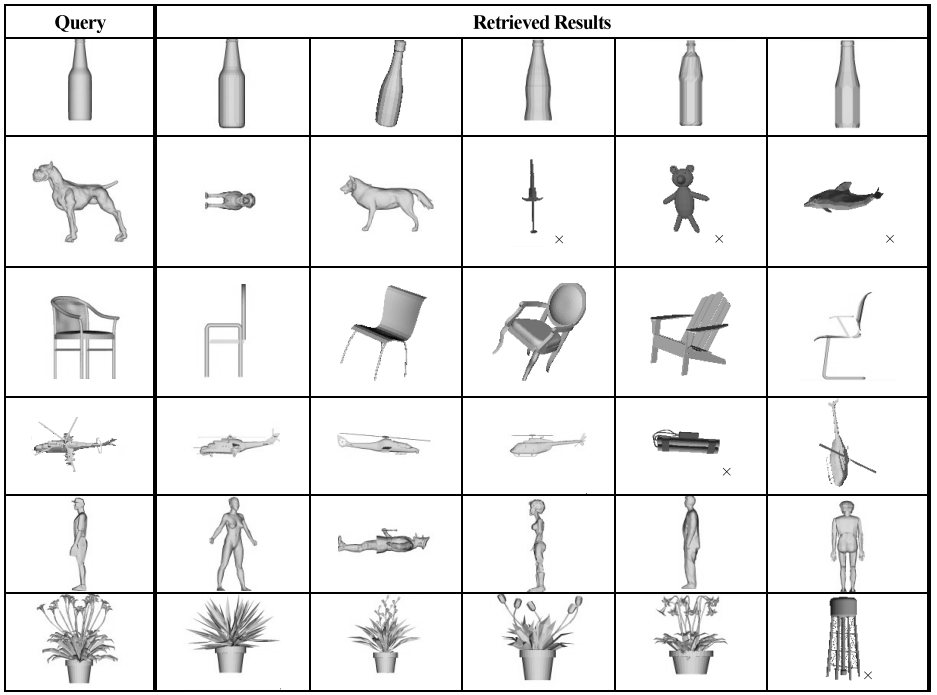

5.3 Parameters Analysis

We tested three resolution levels in Spherical Healpix.

$N_s = 8, 16, 32.$

We computed all the processes except for the last frequency filter procedure (Section 3.7). The power spectrum $|F(u, v)|$ corresponds with the resolution levels. The dimension of the feature vector is

$12 \times n \times n, \quad n = 8, 16, 32.$

From the R-P Curves (see **Fig. 5**) and Average R-P (see **Table 4**), we found that increasing the resolution level improves the retrieval performance. However, the performance decreases if $n \geq 32$.

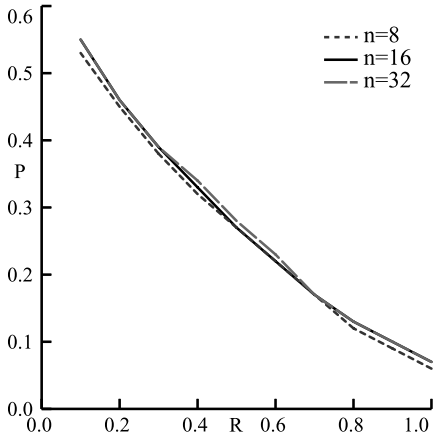

Fig. 5 R-P Curves of different dimensions.

Table 4 Average R-P of different dimensions.

Parameters	Average R-P
$n = 8$	0.261
$n = 16$	0.272
$n = 32$	0.269

We analyzed the causes of this reduction in performance. We conjecture the excessive sampling and division on spherical grid in Spherical Healpix can result in information redundancy. This aspect differs from conventional sampling which requires that the sampling rate must be sufficiently large.

Therefore, we considered using a frequency domain filter to improve the retrieval performance. After performing all the tests on related parameters, we selected $D_0 = n/4$, and $\sigma = 2$ for the condition $n = 32$, and truncated to $n = 8$ to preserve the low frequency components. These settings resulted in the best result, and the dimension of feature vector is given by

$$D_v = 12 \times 8 \times 8 = 768$$

We compared the retrieval effectiveness between the tests with and without a filter, and performance comparison is shown in **Fig. 6** and **Table 5**.

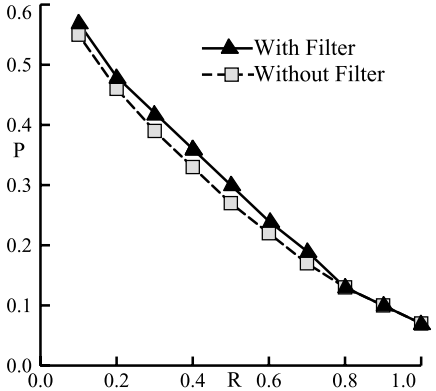

Fig. 6 R-P Curves of filter effect.

Table 5 Average R-P of filter effect.

Parameters	Average R-P
Without Filter	0.269
With Filter	0.286

5.4 Comparison with Other Retrieval Methods on Konstanz Shape Benchmark

We compared our method with the following methods. In (1) and (2), we programmed and implemented the algorithms again, and compared in the same conditions. In (3) and (4), we used the experimental results summarized in Ref. 2) in which (3) and (4) were tested using the same Konstanz Shape Benchmark as our experiment.

(1) **Shape histograms on Shells and Sectors (SSS)** [7]

In this method, the 3D shape can be described as histograms of point fractions belonging to different partitioning shape shells or sectors.

(2) **Shape Distribution (SD)** [5]

This algorithm sampled the probability distribution from the shape surface, and computed a histogram of distances between pairs of points. The similarity between two shapes can be measured from the distribution.

(3) **Rotation Invariant Spherical Harmonics descriptor (RI-SH)** [13]

In this method, firstly, the 3D shape is voxelized into a grid. The spher-

ical function $f_r(\theta, \phi)$ can be described by the intersection of the mesh with the respective voxel. This function is analyzed by Spherical Harmonics Transform to obtain the rotational invariant descriptor.

$$f_r(\theta, \phi) = \sum_{l \geq 0} \sum_{|m| \leq l} f_{l,m} Y_l^m(\theta, \phi) \tag{19}$$

(4) **Rays with Spherical Harmonics (Rays-SH)** [12),14)]

This method was proposed as an improvement of the above-mentioned RI-SH method. In this method, the spherical extent function is defined using the spherical sampling on the grid $2B \times 2B$. The spherical directions u_{ij} are defined as follows.

$u_{ij} = (\theta_i, \phi_j),\ \theta_i = (2i+1)\pi/2B,\ \phi_j = j\pi/B,\ i, j \in [0, 2B-1]$.

The spherical function is defined as $f(\theta_i, \phi_j) = d_{ij}$, and d_{ij} is the largest distance from the center of gravity to the surface of shape in the direction u_{ij}. This spherical function is characterized by spherical harmonics.

$$f(\theta, \phi) = \sum_{l \geq 0} \sum_{|m| \leq l} f_{l,m} Y_l^m(\theta, \phi) \tag{20}$$

The harmonic coefficients $f_{l,m}$ were used for constructing the descriptor.

Here, we refer to our 3D retrieval method based on Spherical Healpix as "SHX". We compared SHX with the four above-mentioned methods on Konstanz Shape Benchmark and show the results for Recall-Precision(R-P) Curves and Average Recall-Precision(R-P) and Average Computation Time on all 3D shapes in **Table 6** and **Fig. 7**.

From the analysis of parameters and comparison with other methods on Konstanz Shape Benchmark, we believe that the SHX method has several advantages over the other methods. At the same time, we discuss the shortfalls of the SHX method.

1) In terms of Average Recall Precision, the SHX method exceeds the other four methods. But results of Rays-SH method are very close to the SHX method.
2) The Recall Precision Curves results indicate that SHX method lies in upper position, especially for Recall $\in [0.1, 0.5]$, and indicates that the SHX has higher retrieval precision than other methods. However, in the Recall $\in [0.8, 1.0]$ region, the performance of the SHX method falls off rapidly.
3) We used 2D Fast Fourier Transform as analysis tool in our algorithm, and its speed is clearly faster than methods based on spherical harmonics. In the other aspect, the sampling is faster than them. For these two reasons, the SHX method is faster than the Rays-SH and RI-SH methods. However, the SHX method is inferior to the SD and SSS statistical methods in terms of computation speed.

Table 6 Comparison of SHX with other methods.

Methods	Average R-P	Average Computation Time
SHX	0.286	80 ms
Rays-SH	0.281	205 ms
RI-SH	0.221	110 ms
SD	0.193	70 ms
SSS	0.171	10 ms

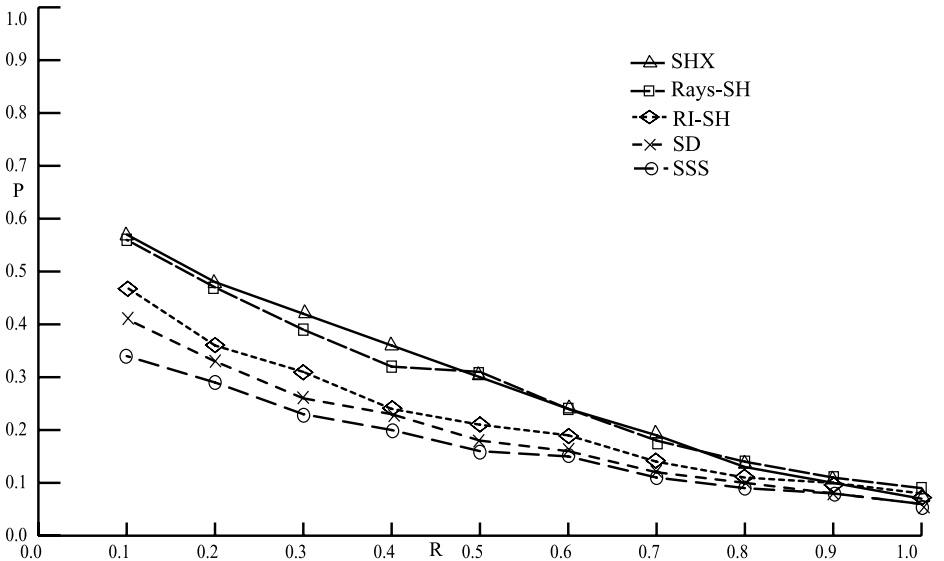

Fig. 7 Comparison of the Recall-Precision Curves of our method "SHX" and other methods.

Table 7 Statistics on SHX method.

Method	NN	First Tier	Second Tier	E-Measure	DCG
SHX	0.58	0.30	0.39	0.23	0.59

Table 8 Statistics on other methods.

Method	NN	First Tier	Second Tier	E-Measure	DCG
RI-SH	0.55	0.29	0.39	0.22	0.57
SD	0.31	0.15	0.21	0.12	0.43
SSS	0.26	0.11	0.17	0.09	0.40

5.5 Evaluate SHX Method on SHREC Data Set

We also evaluated this retrieval method SHX on SHREC data set, in which one collection consists of 1,814 generic 3D models, and has been distributed via the SHREC 2008 website [24].

We computed the quantitative statistics on five recommended parameters [26], Nearest Neighbor (NN), First Tier, Second Tier, E-Measure, Discounted Cumulative Gain (DCG), for evaluation of retrieval results. The statistics in **Table 7** are summarized by averaging these five parameters over all 1,814 shapes in the data set.

We listed the statistics in **Table 8** on the other three methods.

Here the results of SD and SSS are from our implementation, and the descriptor of RI-SH is computed using the executive binary file distributed by the authors of the RI-SH paper (We could not find the details of the implementation or test results on SHREC data set about Rays-SH method. Refer to Section 5.4 about the evaluation of the method on Konstanz Shape Benchmark). Here we will compare RI-SH, SD, and SSS, the three methods with SHX method on SHREC data set.

Through comparing our method with the RI-SH, SD and SSS methods, we found that the SHX descriptor outperforms SD and SSS methods completely, and provides slightly better discrimination than RI-SH descriptor. And SHX descriptor behaves well especially on Nearest Neighbor parameter. This indicates that this SHX descriptor has one advantage, that is, it is easy to help users search one nearest shape belonging to the same class.

Here we show the storage size of SHX feature vector and the average computation time on SHREC data set.

Table 9 Storage size and average computation time of SHX.

Method	Storage size (bytes)	Average Computation Time (s)
SHX	3,072	0.47

Table 10 Storage size and average computation time of other methods.

Method	Storage size (bytes)	Average Computation Time (s)
RI-SH	2,184	0.81
SD	256	0.42
SSS	136	0.18

The storage size of a feature vector is measured by byte. The average computation time, which is shown in **Table 9**, is obtained on a PC with Pentium Core2 Duo-3.0 G processor and 2.0 G memory running Windows XP, and averaging computation time on all the 3D shapes.

We listed the storage size and average computation time on the other three methods in **Table 10**.

We can observe that the SHX method needs more memory storage than all other methods. This is a weakness of SHX method. In the aspect of computation speed, SD and SSS methods belong to statistical methods, and thus have higher speed than SHX method, but SHX is quicker than RI-SH method. It is a future task to find how to reduce the dimensionality of SHX feature vector.

6. Conclusion and Future Work

In this paper, we proposed a 3D shape retrieval method based on Spherical Healpix. We utilized the internal mechanism of Spherical Healpix in this method. We developed a Spherical Healpix Extent Function, projected it onto the Euclidean plane using the inverse-construction of Spherical Healpix, and analyzed it in a frequency domain using the 2 dimensional Fourier transform and the Butterworth low pass filter. The results of the test on Konstanz Shape Benchmark and SHREC data set demonstrated the efficiency of this method. This method is suitable for practical applications because it achieves a good performance and it is easy to help users search one nearest shape belonging to the same class.

In the future, we intend to consider several aspects. Firstly, it is essential to

eliminate pose estimation in the method and find a rotational invariant descriptor using Spherical Healpix. Secondly, we intend to reduce the dimension of the feature vector by employing another frequency domain method. Finally, we also hope to enhance the retrieval performance of the method.

References

1) Funkhouser, T. and Kazhdan, M.: Shape-based retrieval and analysis of 3D models, *SIGGRAPH* Courses (2004).
2) Bustos, B., Keim, A.D., Saupe, D., Schreck, T. and Vranic, D.V.: Feature-based similarity search in 3D object databases, *ACM Computing Surveys*, Vol.37, No.4 (2005).
3) Konstanz Shape Benchmark. http://merkur01.inf.uni-konstanz.de/CCCC
4) Gorski, K.M., Hivon, E., Banday, A.J., Wandelt, B.D., Hansen, F.K., Reinecke M. and Bartelman, M.: HEALPix — A framework for high resolution discretization, and fast analysis of data distributed on the sphere, *Astrophysics*, Vol.622, Issue2, pp.759–771 (2005).
5) Osada, R., Funkhouser, T., Chazelle, B. and Dobkin, D.: Shape distributions, *ACM Trans. Graphics*, Vol.21, No.4 (2002).
6) Ohbuchi, R., Minamitani, T. and Takei, T.: Shape-similarity search of 3D models by using enhanced shape functions, *International Journal of Computer Applications in Technology* (*IJCAT*), Vol.23, No.2/3/4, pp.70–85 (2005).
7) Ankerst, M., Kastenmüller, G., Kriegel, H.P. and Seidl, T.: 3D shape histograms for similarity search and classification in spatial databases, *Proc. 6th International Symposium on Spatial Databases* (1999).
8) Liu, X., Sun, R., Kang, S. and Shum, H.: Directional histogram model for three dimensional shape similarity, *Proc. IEEE international conference on Computer Vision and Pattern Recognition* (2003).
9) Ohbuchi, R., Otagiri, T., Ibato, M. and Takei, T.: Shape-similarity search of three-dimensional models using parameterized statistics, *Pacific Graphics* (2002).
10) Liu, Y., Zha, H. and Qin, H.: The generalized shape distributions for shape matching and analysis, *Proc. IEEE International Conference on Shape Modeling and Applications* (2006).
11) Healy, D.M., Rockmore, D., Kostelec, P. and Moore, S.: FFTs for the 2-sphere improvements and variations, TR2002-419, Dartmouth College (2002).
12) Vranic, D.V., Saupe, D. and Richter, J.: Tools for 3D-object retrieval: Karhunen–Loeve transform and spherical harmomics, *Proc. IEEE Workshop on Multimedia Signal Processing* (2001).
13) Funkhouser, T., Min, P., Kazhdan, M., Chen, J., Halderman, A., Dobkin, D. and Jacobs, D.: A search engine for 3D models, *ACM Transactions on Graphics*, Vol.22, No.1, pp.83–105 (2003).
14) Vranic, D.V.: An improvement of rotation invariant 3D shape descriptor based on functions on concentric spheres, *Proc. IEEE International Conference on Image Processing*, Vol.3, pp.757–760 (2003).
15) Saupe, D. and Vranic, D.V.: 3D model retrieval with spherical harmonics and moments, *Proc. DAGM* (2001).
16) Vranic, D.V. and Saupe, D.: Description of 3D-shape using complex function on the sphere, *Proc. IEEE International Conference on Multimedia* (*ICME*) (2002).
17) Novotni, M. and Klein, R.: 3D Zernike descriptors and content based shape retrieval, *Proc. ACM Symposium on Solid Modeling and Applications* (2003).
18) Podolak, J., Shilane, P., Golovinskiy, A., Rusinkiewicz, S. and Funkhouser, T.: A Planar-Reflective Symmetry Transform for 3D Shapes, *ACM Trans. Graphics* (*SIGGRAPH2006*), Vol.25, No.3 (2006).
19) Bespalov, D., Ip, C.Y., Regli, W.C. and Shaffer, J.: Benchmarking CAD search techniques, *Proc. ACM Symposium on Solid and Physical Modeling* (2005).
20) Paquet, E., Rioux, M., Murching, A., Naveen, T. and Tabatabai, A.: Description of Shape Information for 2-D and 3-D Objects, *Signal Processing: Image Communication*, Vol.16, No.1-2 (2000).
21) Chen, D.Y. and Ouhyoung, M.: A 3D Model Alignment and Retrieval System, *Proc. International Computer Symposium* (2002).
22) Jolliffe, I.T.: Principal Component Analysis, Springer (1986).
23) Gonzalez, R.C. and Woods, R.E.: *Digital Image Processing*, Second Edition, Prentice Hall, Chapter4 (2002).
24) http://www.kki.yamanashi.ac.jp/˜ohbuchi/research/SHREC/index.html
25) Liu Z., Mitani J., Fukui, Y. and Nishihara, S.: Multiresolution wavelet analysis of shape orientation for 3D shape retrieval, *ACM International Conference on Multimedia Information Retrieval* (*Proc. ACM Multimedia*) (2008).
26) Shilane, P., Min, P., Kazhdan, M. and Funkhouser, T: The princeton shape benchmark, *Proc. Shape Modeling International* (2004).

(Received October 4, 2007)
(Accepted September 10, 2008)
(Released December 10, 2008)

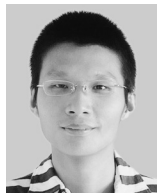

Zhenbao Liu received his Master and Bachelor degrees from Northwestern Polytechnical University, China, in 2004 and 2001, respectively. He is now pursuing a doctor's degree at Department of Computer Science, Graduate School of Systems and Information Engineering, University of Tsukuba, Japan. His research interests include computer graphics, shape processing, and data retrieval.

Jun Mitani received his Master and Ph.D. degrees from The University of Tokyo, Japan, in 2000 and 2004 respectively. He joined Riken as a researcher in 2004. He is currently a lecturer at Department of Computer Science, University of Tsukuba, Japan. His research interests include computer graphics, design aid of paper model, origami. He is also a Presto researcher of Japan Science and Technology Agency. He is a member of Japan Society of Graphics Science, Society for Art and Science of Japan.

Yukio Fukui received his Doctor, Master and Bachelor degrees from The University of Tokyo, University of Tokyo, and Kyoto University in 1993, 1980 and 1973, respectively. After graduation of master, he joined Agency of Industrial Science and Technology, Ministry of International Trade and Industry. He served as a research director in National Institute of Bioscience and Human-Technology from 1993. He is currently a professor at Department of Computer Science, University of Tsukuba from 1998. His research interests include shape processing, optical CAD system, shape design system, virtual reality. He is a member of Information Processing Society of Japan, Virtual Reality Society of Japan, Human Interface Society, Japan Ergonomics Society, Japanese Society of Ophthalmological Optics, and ACM.

Seiichi Nishihara graduated from Department of Mathematics and Engineering, Kyoto University, Japan, in 1968. And in the same year, he served as an assistant in Center of Large Scale Computer Systems, Kyoto University, Japan. He is currently a professor of Department of Computer Science, University of Tsukuba. His research interests include constraint satisfaction problem, production of virtual city. He is a member of Information Processing Society of Japan, Japanese Society for Artificial Intelligence. He is also the president of Society for Art and Science of Japan.